J. Phys. D: Appl. Phys. **42** (2009) 105410 (6pp) doi:10.1088/0022-3727/42/10/105410

Investigations on the structural, optical and electronic properties of Nd doped ZnO thin films

M Subramanian[1], P Thakur[2], S Gautam[2], K H Chae[2], M Tanemura[1], T Hihara[3], S Vijayalakshmi[4], T Soga[1], S S Kim[5], K Asokan[5,6] and R Jayavel[4,7]

[1] Department of Frontier Materials, Graduate School of Engineering, Nagoya Institute Technology, Gokiso-cho, Showa-ku, Nagoya 466-8555, Japan
[2] Materials Science and Technology Research Division, KIST, Seoul 136-791, Korea
[3] Department of Materials Science and Engineering, Nagoya Institute Technology, Gokiso-cho, Showa-ku, Nagoya 466-8555, Japan
[4] Crystal Growth Centre, Anna University, Chennai 600 025, India
[5] School of Materials Science and Engineering, Inha University, Incheon, Korea
[6] Inter-University Accelerator Centre, Aruna Asaf Ali Marg, New Delhi 110 067, India
[7] Centre for Nanoscience and Technology, Anna University, Chennai, 600 025, India

E-mail: subu_cgc@yahoo.com and rjvel@annauniv.edu

Received 29 January 2009, in final form 11 March 2009
Published 29 April 2009
Online at stacks.iop.org/JPhysD/42/105410

Abstract
We report the synthesis and characterization of Nd doped ZnO thin films grown on Si (1 0 0) substrates by the spray pyrolysis method. The surface morphology of these thin films was investigated by scanning electron microscopy and shows the presence of randomly distributed structures of nanorods. Grazing angle x-ray diffraction studies confirm that the doped Nd ions occupied Zn sites and these samples exhibited a wurtzite hexagonal-like crystal structure similar to that of the parent compound, ZnO. The micro-photoluminescence measurement shows a decrease in the near band edge position with Nd doping in the ZnO matrix due to the impurity levels. The near-edge x-ray absorption fine structure (NEXAFS) measurements at the O K edge clearly exhibit a pre-edge spectral feature which evolves with Nd doping, suggesting incorporation of more charge carriers in the ZnO system and the presence of strong hybridization between O 2p–Nd 5d orbitals. The Nd M_5 edge NEXAFS spectra reveal that the Nd ions are in the trivalent state.

(Some figures in this article are in colour only in the electronic version)

1. Introduction

Among the II–VI functional semiconductor materials, zinc oxide (ZnO) has attracted significant interest because of its novel properties such as direct wide band gap, large exciton binding energy, high chemical stability and environment-friendly applications [1]. It has importance both in basic and applied research because of its unique properties such as catalytic, optical, electrical, optoelectronic, gas-sensing, piezoelectric and photoelectrochemical nature [2, 3]. At the same time, the methods for introducing new magnetic, optical, electronic, photo-physical or chemical properties to these semiconductor hosts are attracting intense interest as prospects for technological applications emerge in the areas of spintronics [4], optoelectronics [5], quantum computing [6], photocatalysis [7] and luminescence materials [8]. One of the effective methods for manipulating the physical properties of semiconductors is doping the impurity ions. It has been proved that the physical and chemical properties are greatly influenced by doping of the foreign metals in the host ZnO lattice. For example, in the field of spintronics, transition metal doped ZnO provides efficient injection of spin-polarized carriers. Recent experiments have shown that the introduction of rare-earth metals (REMs) such as Gd ion in

wide band-gap semiconductor, GaN, results in ferromagnetic property with the magnetic moment of 4000 μ_B/Gd atom [9]. This has motivated the researchers on REM ion doping in ZnO for spintronic applications. Potzger *et al* studied the magnetic properties of Gd implanted ZnO single crystals [10]. The REM ions have the advantage of possessing very high orbital momentum leading to high total magnetic moments per atom, for example 7 μB for Gd and 3.27 μB for Nd. It also has potential applications as visible light emitting phosphors in displays, high power lasers and other optoelectronic devices [11–13].

Recently, Ungureanu *et al* [14] studied the electrical and magnetic properties of Nd doped ZnO thin films and showed that the resistivity of Nd doped ZnO reduces by increasing the thickness of the film. Qingyu Xu *et al* investigated the co-doping of Nd and Mn ions in the ZnO matrix and showed the room temperature (RT) ferromagnetism. It was also suggested that co-doping of Nd ions in the Mn doped ZnO is one of the possible ways to introduce new energy levels in the band gap and to mediate the electron spins of the magnetic dopants [15]. Previous reports on Nd doped ZnO (i.e. $Zn_{1-x}Nd_xO$) focused on the luminescence, magnetic and electrical properties. Band gap was tailored by doping of Nd ions in TiO_2 for photovoltaic and visible photocatalytic applications [16]. Xie and Yuan demonstrated that Nd doped TiO_2 possesses photocatalytic property under visible light irradiation [17]. Detailed literature survey shows that there are a very few reports on the systematic studies of Nd doping in ZnO [14]. With this motivation, Nd was doped into ZnO matrix by spray pyrolysis method on the Si(1 0 0) substrate and the investigation was done to understand the band-gap variation and identification of the valence states of Nd ions in the films. Photoluminescence (PL) and near-edge x-ray absorption fine structure (NEXAFS) are very powerful tools, respectively, for understanding their optical and electronic structural properties of these materials.

Present investigation is focused on synthesis of Nd doped ZnO thin films and characterization by various experimental techniques to understand their structural, magnetic, optical properties and electronic structure.

2. Preparation of Nd doped ZnO

The thin films of $Zn_{1-x}Nd_xO$ ($x = 0$, 0.03, 0.05, 0.07, 0.10 and 0.15) were deposited by using a spray pyrolysis technique. Zinc acetate ($Zn(CH_3COO)_2 \cdot 2H_2O$) and neodymium acetate hydrate ($Nd(CH_3CO_2)_3 \cdot xH_2O$) were used as precursors for Zn and Nd, respectively. Initially, $Zn(CH_3COO)_2 \cdot 2H_2O$ was dissolved in de-ionized water (resistivity of the water is 18.2 MΩ cm) and stirred for half an hour at RT, which was used as a spray solution for ZnO thin films. For Nd doping, stoichiometric amount of $(Nd(CH_3CO_2)_3$ was dissolved in de-ionized water separately and mixed with the starting solution as a drop wise addition, and then stirred continuously for 2 h at RT to get a homogeneous solution. The total concentration of the solution was kept as 0.5 mol. The films were deposited on ultrasonically cleaned Si(1 0 0) substrates. Before deposition, the substrates were heated up to 400 °C and all films were deposited at 400 °C. Compressed air was used as the carrier gas; the airflow rate was maintained at 40 lbs in^{-2}. The distance between the spray nozzle and the substrate is 30 cm. The solution was sprayed on the substrates for several spraying cycles of 3 s duration, followed by an interval of 1 min, to avoid the strong cooling of the substrate due to continuous spray. The films were sprayed for 45 min with the above explained systematic steps and thickness of the films was ≈140 nm as determined by using a profilometer.

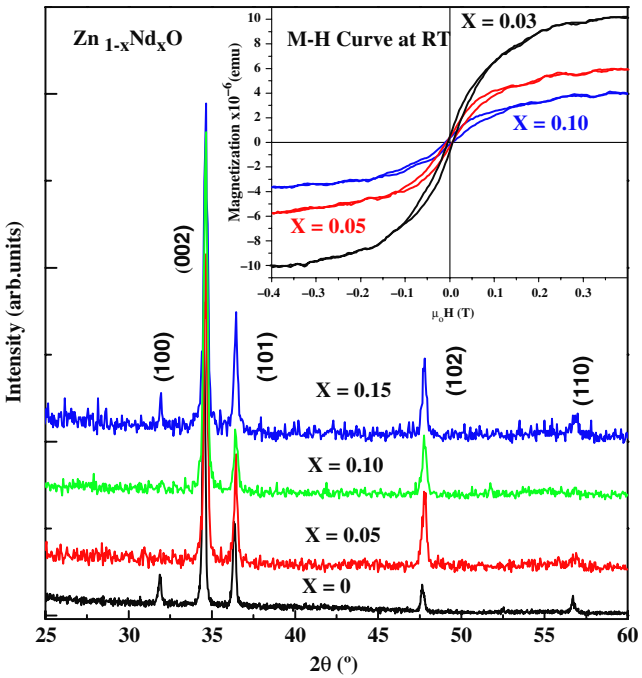

Figure 1. Grazing angle XRD patterns for $Zn_{1-x}Nd_xO$ thin films show the single phase formation for various Nd concentrations. Inset shows the hysteresis loop (M–H curve) of $Zn_{1-x}Nd_xO$ thin films measured at RT.

3. Results and discussion

3.1. Structural and magnetic characterizations

Grazing angle x-ray diffraction (GXRD) studies were performed to understand the crystal structure. To record the x-ray diffraction (XRD) patterns, the grazing angle geometry was used with Cu K_α radiation. Measurements were performed at an incidence angle of 0.5° and the typical XRD patterns were recorded for 2θ varying from 20° to 60° using a Bruker D8 discover x-ray diffractometer. The GXRD patterns of $Zn_{1-x}Nd_xO$ thin films coated on the Si (1 0 0) substrates are shown in figure 1. It is clear that these films were of polycrystalline nature and diffraction peaks revealed the hexagonal wurtzite structure without any secondary phases. It was also evident that all the films exhibit preferential c-axis orientation due to the lowest surface free energy of the (0 0 2) plane [18]. From the XRD patterns, it was observed that the (0 0 2) position shifts towards the higher angle side with increasing Nd dopant level in the ZnO thin films. This information allows one to obtain the change in lattice constant of $Zn_{1-x}Nd_xO$ thin films. From the XRD measurement,

the c-axis length was calculated by equation (1) using the diffraction peak position of the (0 0 2) plane [19].

$$c = \frac{\lambda}{\sin\theta}, \tag{1}$$

where λ is the wavelength and θ is the Bragg diffraction angle in degree. The calculated values of the c-axis lengths were 5.2084, 5.1691, 5.1662 and 5.1705 for $x = 0$, 0.05, 0.10 and 0.15, respectively. It was observed that the c-axis length decreases with increasing Nd concentration. This is attributable to Nd ions occupying the Zn sites that are in tetrahedrally coordinated in the wurtzite crystal structure. Decreasing the c-axis can be explained by the following approach: when the Nd^{3+} ions occupy the substitutional position of Zn^{2+} ions then cationic vacancies could be created due to the electrical neutrality of ZnO crystal and it was shown by the mechanism given below:

$$3Zn^{2+} \rightarrow 2Nd^{3+} + V_{Zn}^{2+} \tag{2}$$

This can be rewritten by using the Kröger–Wink notation,

$$0 = 2Nd_{Zn'} + V_{Zn'}. \tag{3}$$

Thus induced cationic vacancies created by Nd^{3+} doping in the ZnO host matrix are responsible for the decrease in the c-axis length. Similar c-axis variations were also reported in Er doped ZnO [11] and Ce doped ZnO [20]. The shift in the peak position towards higher angle side and the decrease in the c-axis length indicate that when the Nd ions are replacing the Zn ions the tensile stress and structural defects were introduced in the host lattice. It was also noted that the FWHM increases with increasing Nd concentration and this implies decrease in the crystalline quality.

To investigate the magnetic properties of the $Zn_{1-x}Nd_xO$ thin films, isothermal magnetization hysteresis measurements were performed at RT using alternating gradient force magnetometer (AGFM) (MicroMag-2900, Princeton Measurements Co.) with a sensitivity of 10^{-8} emu. The inset in figure 1 shows magnetization versus magnetic field (M–H) curves for $Zn_{1-x}Nd_xO$ ($x = 0.03$, 0.05 and 0.10) thin films. As evident, all these films exhibit a well-defined magnetization hysteresis implying the ferromagnetic behaviour at RT.

3.2. Film composition and surface analysis

A tandetron accelerator with 2 MeV $4He^+$ particles and a current of 15 nA was used for Rutherford backscattering (RBS) measurements. The backscattered particles were detected at an angle of 165° with respect to the incident beam direction by a surface barrier detector. The stoichoimetry of the films were derived from the experimental data by simulating theoretically by using software called GISA 3. Figure 2 shows the RBS spectra of 5% and 15% Nd doped ZnO thin films, which clearly shows that the Nd signal increases with Nd concentrations. The composition of $Zn_{0.95}Nd_{0.05}O$ and $Zn_{0.85}Nd_{0.15}O$ was calculated from the RBS results and match well with the chemical stoichoimetry. Figures 3(a) and (b) show the scanning electron microscopy (SEM) images of the undoped and 15 mol% Nd doped ZnO thin films, respectively. A random distribution of horizontally aligned nanorods spread on the uniform $Zn_{1-x}Nd_xO$ nanocrystalline surface is clearly seen in SEM images. The average length of the nanorods was found to be ~10–15 μm.

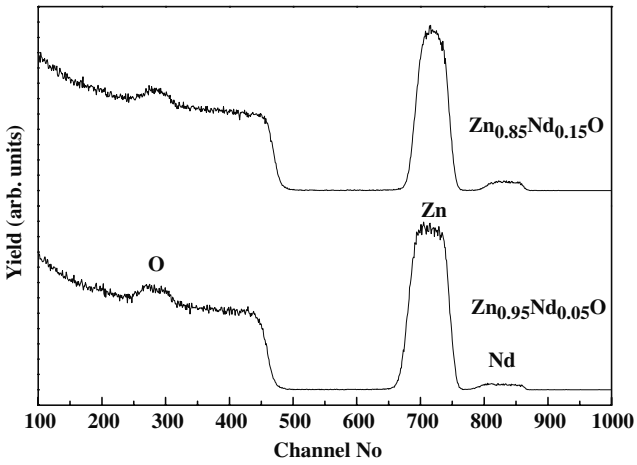

Figure 2. Rutherford backscattering spectra of $Zn_{0.95}Nd_{0.05}O$, and $Zn_{0.85}Nd_{0.15}O$ films show that the Nd signals increases with Nd concentrations.

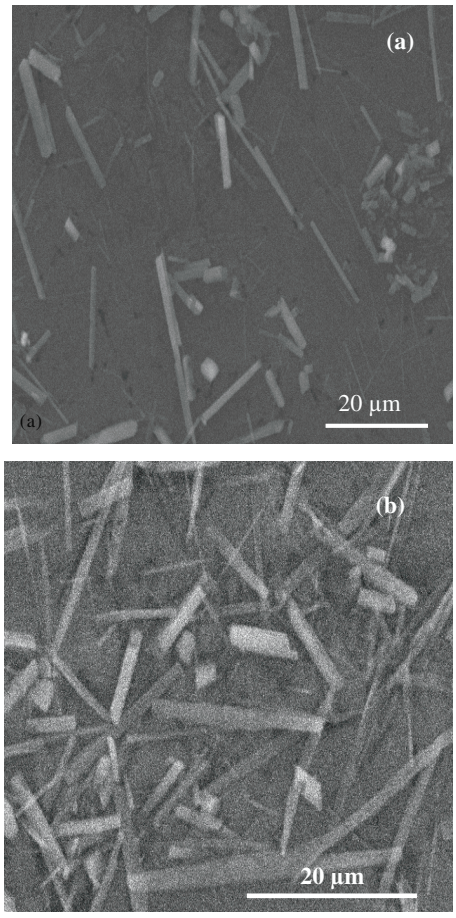

Figure 3. SEM images for (a) ZnO and (b) $Zn_{0.85}Nd_{0.15}O$ thin films. The size of the nanorods is ~10–15 μm.

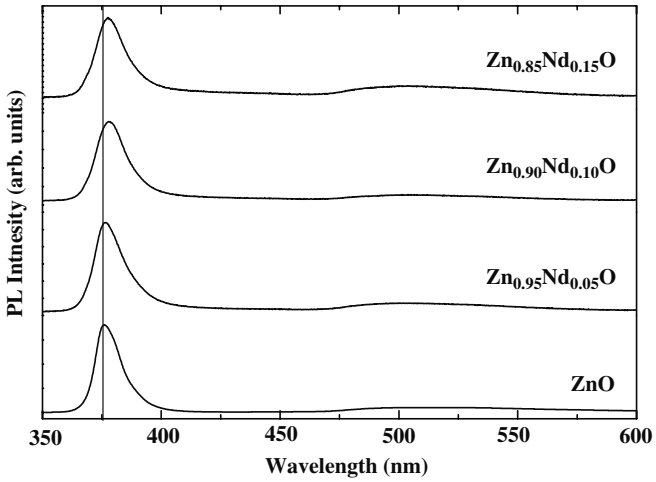

Figure 4. PL spectra for $Zn_{1-x}Nd_xO$ thin films and the variation of near band edge position shift are indicated by the vertical line.

3.3. PL studies

In order to study the influence of Nd doping on the optical properties of the films, PL measurements have been carried out. PL spectra were recorded using He–Cd laser (325 nm) as the light source for optical pumping. Figure 4 shows the PL spectra of $Zn_{1-x}Nd_xO$ thin films collected at RT. The observed spectral features were divided into two regions; (a) the peak centred at ∼374 nm can be attributed to the bound exciton transitions [21] and (*b*) the broad region around 500 nm can be assigned to the deep-level emissions, i.e. the green and red emissions. However, the interpretation of deep-level emissions (region around 500 nm) is still controversial because of defects in ZnO. In general, it is widely accepted that the deep-level emissions are closely related to the structural defects such as oxygen vacancies or Zn interstitials in the ZnO [22–26]. It is clear from figure 4 that the band edge position of $Zn_{1-x}Nd_xO$ is shifted towards higher wavelength with Nd substitution. This is directly related to the introduction of new unoccupied states by Nd 4f electrons that are located close to the lower edge of conduction band of the ZnO energy levels. Table 1 shows the near band edge positions calculated from the micro PL measurements. A similar band edge variation was observed in Nd doped TiO_2 samples and was attributed to the introduction of new electronic states (unoccupied orbitals) by substitutional Nd^{3+} ions in TiO_2 [16, 17]. These results are also consistent with other studies where REM ions such as Er^{3+} doped in ZnO thin films. This study shows that the variation in band edge position is due to the some donor levels produced by the partially filled 4f states of Er [27]. Similar results were also reported for Cd doped ZnO [28] and Ce doped ZnO [20]. Apart from the band edge position shift, the intensity of the band edge peak is decreased considerably with Nd doping (see table 1). A continuous decrease in intensity indicates that the decrease in crystalline quality of $Zn_{1-x}Nd_xO$ thin films which is consistent with GXRD results.

3.4. NEXAFS studies

To understand the electronic structure of unoccupied states of $Zn_{1-x}Nd_xO$ thin films, the NEXAFS experiments were carried

Table 1. Near band edge position and PL intensity of $Zn_{1-x}Nd_xO$ films determined by micro-PL measurement.

Concentration of Nd (mol%)	Near band edge position (nm)	PL Intensity (cps)
0	376	2 57 123
5	377	9 746
10	378	8 964
15	378	6 123

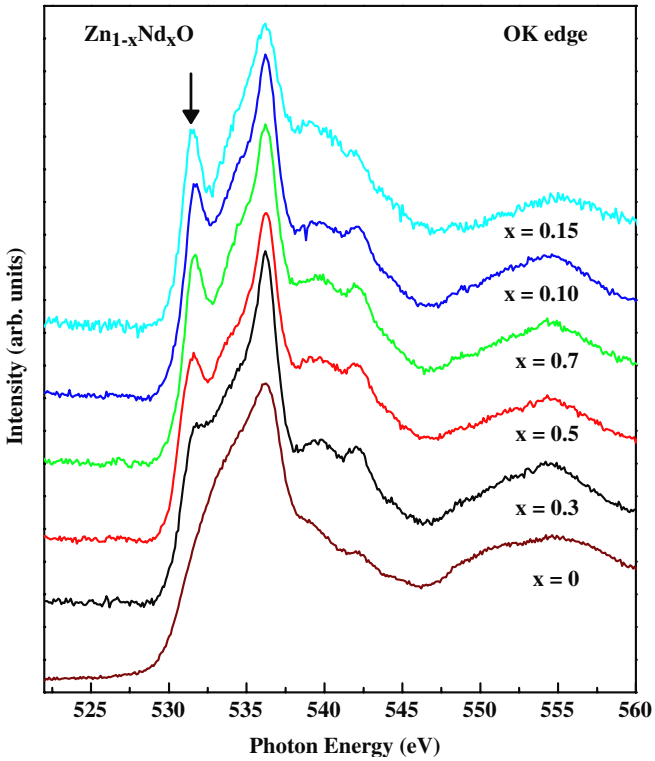

Figure 5. NEXAFS spectra at O K edges for $Zn_{1-x}Nd_xO$ thin films and the evolution of pre-edge peak is marked by an arrow. The intensity of this pre-edge peak increases with Nd concentration.

out at O K edge and Nd M_5 edges. These experiments were performed at the soft x-ray beamline 7B1 XAS KIST of the Pohang Light Source, operating at 2.5 GeV with a maximum storage current of 200 mA. All scans were collected in total-electron yield (TEY) mode at RT and the base pressure of the experimental chamber was better than 1.5×10^{-8} Torr. All spectra were normalized to the incident photon flux.

Figure 5 shows the normalized O K edge NEXAFS spectra of $Zn_{1-x}Nd_xO$ acquired at RT in TEY mode. These spectra correspond to the O 1s to 2p dipole transitions. For metal oxides, the spectral features at O K edge arise from the covalent mixing of the metal and the oxygen states and corresponds to unoccupied states of metallic character making the O (1s)-metal (d,s,p) electronic transitions that are dipole allowed [29–31]. As evident from figure 5, the pre-edge peak at ∼531 eV evolves with Nd doping in ZnO (shown in figure 5 by an arrow) and its intensity increases with Nd concentrations. This pre-edge feature carries a substantial amount of information. Similar pre-edge features have been reported in the oxides mainly in cuprates and manganites [29, 30]. Recently the similar pre-edge peak was observed

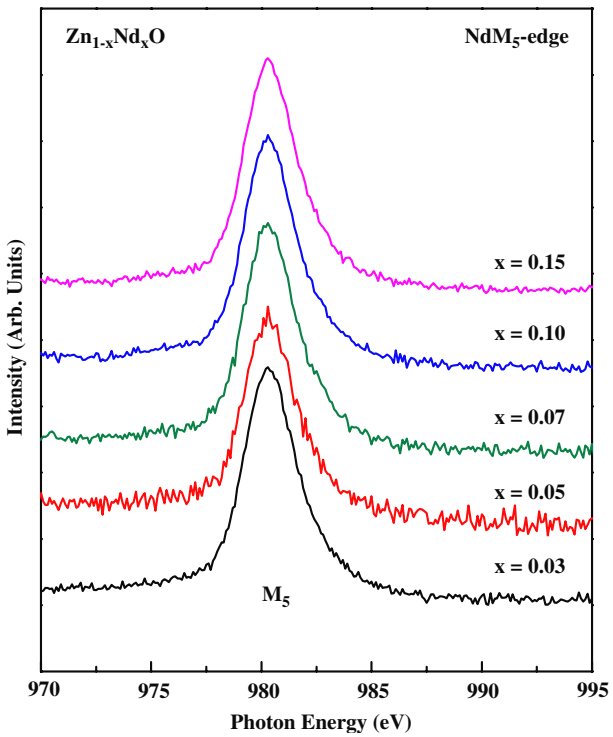

Figure 6. NEXAFS spectra at Nd M_5 edge for $Zn_{1-x}Nd_xO$ thin films for various concentrations. These spectra indicate that the Nd valence state is 3+.

in Mn doped ZnO [32]. Since this feature originates from Nd doping, it is ascribed to dipole transitions from O 1s to O 2p states that are hybridized with the unoccupied states and reflects the presence of more charge carriers: electrons or holes. This clearly suggests that Nd ions are incorporated in the system and responsible for change in their electronic structures. Based on existing literatures, the spectral features are assigned as follows: (*a*) the energy region between 530 and 539 eV is attributed mainly to O 2p hybridization with highly dispersive Zn 3d4s/Nd 5d states, which form the bottom of the conduction band with a peak at ∼536 eV due to transition to non-dispersive O 2p states, and (*b*) the region between 539 and 550 eV is assigned to O 2p hybridized with Zn 4p/Nd 5d6s states and above 550 eV the spectrum arises due to the O 2p states that extend Zn/Nd higher orbitals.

Rare-earth ions such as Nd exist in a stable trivalent state in many compounds. The NEXAFS at M_5 edge probes directly the inner 4f configuration. These edges exhibit sharp final-state multiplets that serve as finger prints of the 4f configuration as these reproduce unambiguously the localized nature of the 4f configuration [31, 33–35]. Figure 6 displays the NEXAFS spectra at M_5-edge of Nd doped ZnO in TEY mode at RT. Since there is no change in the spectral features or additional multiplet structure at Nd M_5-edge with Nd doping in ZnO, suggesting that valence state of Nd ion remains in trivalent state.

Above study described the synthesis and characterization of Nd doped ZnO thin films. All these thin films were polycrystalline and exhibit RT ferromagnetic property. The results from NEXAFS study show strong evidence for hybridization of Nd ions with O ions in the ZnO lattice. It also provides the information that trivalent Nd ions occupies divalent Zn site resulting in more charge carriers. These experimental results show that Nd doped ZnO thin films are suitable for spintronics applications.

4. Conclusion

Nd doped ZnO thin films were prepared by spray pyrolysis and GXRD studies revealed the polycrystalline nature of these films with wurtzite structure. Magnetic measurements confirmed that Nd doped ZnO samples exhibit ferromagnetic properties at RT. From the micro-PL studies, it is observed that the near band edge position of Nd doped ZnO shifts towards the higher wavelength side due to the substitution of Nd ions. The NEXAFS spectra of $Zn_{1-x}Nd_xO$ at the O K edge shows an evolution of pre-edge spectral feature similar to cuprates and manganites, and also confirms the strong hybridization of O 2p–Nd 5d states. The NEXAFS spectra at the Nd M_5 edge provide evidence that Nd ions are in the trivalent state.

Acknowledgments

One of the authors (MS) would like to acknowledge the Japanese Government for providing the Monbukagakusho fellowship. The authors acknowledge Professor Ajay Gupta and Dr V R Reddy, UGC-DAE-Consortium for Scientific Research, Indore for GXRD measurements.

References

[1] Cheng C, Xin R, Leng Y, Yu D and Wong N 2008 *Inorg. Chem.* **47** 7868
[2] Yao K X and Zeng H C 2006 *J. Phys. Chem.* B **110** 14736
[3] Wang Z L and Song J H 2006 *Science* **312** 242
[4] Wolf S A, Awschalom D D, Buhrman R A, Daughton J M, von Molnár S, Roukes M L, Chtchelkanova A Y and Treger D M 2001 *Science* **294** 1488
[5] Shim M, Wang C, Norris D J and Guyot-Sionnest P 2001 *MRS Bull.* **26** 1005
[6] Golovach V N and Loss D 2002 *Semicond. Sci. Technol.* **17** 355
[7] Kudo A and Sekizawa M 2000 *Chem. Commun.* 1371
[8] Chan W C W and Nie S 1998 *Science* **281** 2016
[9] Dhar S, Brandt O, Ramsteiner M, Sapega V F and Ploog K H 2005 *Phys. Rev. Lett.* **94** 037205
[10] Potzger K, Shengqiang Z, Eichhorn F, Helm M, Skorupa W, Mücklich A, Fassbender J, Herrmannsdörfer T and Bianchi A 2006 *J. Appl. Phys.* **99** 063906
[11] Pérez-Casero R, Gutiérrez-Llorente A, Pons-Y-Moll O, Seiler W, Defourneau R M, Defourneau D, Millon E, Perrière J, Goldner P and Viana B 2005 *J. Appl. Phys.* **97** 054905
[12] John J S and Coffer J L 2000 *Appl. Phys. Lett.* **77** 1635
[13] Deng R, Zhang X T, Zhang E, Liang Y, Liu Z, Xu H, Hark S K J 2007 *Phys. Chem.* C **111** 13013
[14] Ungureanu M, Schmidt H, Xu Q, von Wenckstern H, Spemann D, Hochmuth H, Lorenz M and Grundmann M 2007 *Superlatt. Microstruct.* **42** 231
[15] Xu Q, Schmidt H, Hochmuth H, Lorenz M, Setzer A, Esquinazi P, Meinecke C and Grundmann M 2008 *J. Phys. D: Appl. Phys.* **41** 105012
[16] Li W, Wang Y, Lin H, Ismat Shah S, Huang C P, Doren D J, Rykov S A, Chen J G and Barteau M A 2003 *Appl. Phys. Lett.* **83** 4143

[17] Xie Y and Yuan C 2004 *Appl. Surf. Sci.* **221** 17
[18] Chopra K, Major S and Pandaya D 1983 *Thin Solid Films* **102** 1
[19] Cullity B D 1978 *Elements of X-Ray Diffraction* 2nd edn (Reading, MA: Addison-Wesley)
[20] Sofiani Z, Derkowska B, Dalasiński P, Wojdyła M, Dabos-Seignon S, Alaoui Lamrani M, Dghoughi L, Bała W, Addou M and Sahraoui B 2006 *Opt. Commun.* **267** 433
[21] Harako S, Yokoyama S, Ide K, Zhao X and Komoro S 2008 *Phys. Status Solidi* a **205** 19
[22] Vanheusden K, Warren W L, Seager C H, Tallant D R, Voigt J A and Gnade B E 1996 *J. Appl. Phys.* **79** 7983
[23] Li Y, Cheng G and Zhang L 2000 *J. Mater. Res.* **15** 2305
[24] Studenikin A, Golego N and Cocivera M 1998 *J. Appl. Phys.* **84** 2287
[25] Ko H J, Yao T, Chen Y and Hong S K 2002 *J. Appl. Phys.* **92** 4354
[26] Koida T, Chichibu S F, Uedono A, Tsukazki A, Kawasaki M, Sota T, Segawa Y and Koinuma H 2003 *Appl. Phys. Lett.* **82** 532
[27] Choi M H and Ma T Y 2008 *Mater. Lett.* **62** 1835
[28] Wang Y S, John Thomas P and O'Brien P 2006 *J. Phys. Chem.* B **110** 21413
[29] Pellegrin E *et al* 1993 *Phys. Rev.* B **47** 3354
[30] Asokan K *et al* 2004 *J. Phys.: Condens. Matter.* **16** 3791
[31] Asokan K, Dong C L, Bao C W, Tsai H M, Chiou J W, Chang C L, Pong W F, Duran P, Moure C and Peña O 2005 *Solid State Commun.* **134** 821
[32] Thakur P, Chae K H, Kim J-Y, Subramanian M, Jayavel R and Asokan K 2007 *Appl. Phys. Lett.* **91** 162503
[33] Hu X H, Blythe H J, Ziese M, Behan A J, Neal J R, Mokhtari A, Ibrahim R, Kenji U, Hitoshi T and Tomoji K 2001 *Appl. Phys. Lett.* **79** 988
[34] Bonnelle C, Karnatak R C and Spector N 1977 *J. Phys. B: At. Mol. Phys.* **10** 795
[35] Isnard O, Miraglia S and Buschow K H J 1997 *Physica* B **239** 365